Dereje Berihun Sitotaw[1]*
Dustin Ahrendt[2]
Yordan Kyosev[2]
Abera Kechi Kabish[1]

Investigation of Stab Protection Properties of Aramid Fibre-Reinforced 3D Printed Elements

[1] Bahir Dar University, Ethiopian Institute of Textile and Fashion Technology,
Bahir Dar, 6000, Ethiopia,
* e-mail: dereje.berihun@bdu.edu.et,
e-mail: abera.kechi@bdu.edu.et

[2] TU Dresden, Institute of Textile Machinery and High Performance Material Technology, Chair of Development and Assembling of Textile Products,
01062, Dresden, Germany,
e-mail: dustin.ahrendt@posteo.de,
e-mail: yordan.kyosev@tu-dresden.de

Abstract

A stab resistant vest is a reinforced piece of body armour designed to resist knife or needle attacks of different energy levels specifically to the upper part of the body (chest and abdomen) to save lives. The majority of armours limit several comfort parameters, such as free locomotion, respiration, flexibility and light weight, which determine efficient use by wearers and their willingness to wear. Currently available armours are usually made of a single plate, and although often segmentation is used with just a few but still quite large pieces, the materials are compact and bulky to wear. In this study, stab protective armor elements (scale-like elements) of 3 mm thickness and 50 mm diameter were designed, produced (3D printed) and tested for performance. Aramid fibre was used for its strength, durability and process ability to develop protection elements at unidirectional and multidirectional filling angles during 3D printing. The specimens were tested according to VPAM KDIW 2004. The specimens designed and developed with multidirectional filling angles of aramid resist the puncturing energy level K1 (25 J) with a penetration depth less than the maximum allowed for the K1 energy level by VPAM. These specimens showed a high protection level of relative small thickness (3 mm) and light weight (6.57 grams for the estimated area $A \approx 1963.5$ mm²) as compared to the currently certified armors for K1 (for example, the aluminum mass is 13.33 grams for 2 mm thickness and 50 mm diameter).

Key words: *stab protection armor, 3D printing, printed scales, impact energy, penetration depth, fibre-reinforcement, aramid.*

Introduction

Protective clothing is one of the most important pieces of safety equipment to save lives. A stab resistant vest is a reinforced piece of body armor designed to resist knife or needle attacks specifically to the upper part of the body (chest, back and sides), and it can be worn either as covert or overt.

Early humans used comparatively primitive armors which were manufactured out of metal, horn, wood or leather lamellae [1, 2], but as civilisations evolved and knowledge advanced, body armor was introduced. Then in the last century, with its two world wars, various attempts were made to advance the technology of body armor [1]. It was reported that the first soft body armor was developed by the Japanese, which was made of silk and was most effective against low-velocity bullets [3]. Then, the first so-called bullet-proof vests were designed in America in the two decades following World War I [4, 5] while modern police body armor was introduced into practice in the 1970s [6].

Police officers, the military, as well as transport and correction administrators should encourage their staff to wear stab vests during the whole duty shift to save them from a fatal injury if stabbed in the torso [7]. The level of protection required in soft and sensitive bodily regions is determined by the types of attacks that are likely to be encountered [8]. The design of appropriate stab vests with the desired level of protection can be challenging for the wide range of weapons which are used for puncturing, and stabbing techniques are different depending on the assailant [9].

Although protection and comfort are conflicting, body armors for stab protection should also consider flexibility [10] and other ergonomic issues for acceptance along with coverage and duration [11-13].

The selection of advanced materials (both for performance and comfort) and appropriate armor design should ideally allow the flow of excessive metabolic heat away from the body (thermo-physiological property), which can be reflected by a combination of air permeability, thermal resistance, and moisture evaporation [14-16]. The garment should be able to transfer heat and moisture away from the skin to the atmosphere [16-18]. Tactile comfort, the feel or sensation on the skin when worn, should be considered during the design of protection gear [19, 20].

The use of body armor has always been an issue when the ease of body movement and cognitive functions are considered [21, 22] and should not be drastically compromised by the design of the body armor [13].

Many biological systems possess hierarchical and fractal-like interfaces and joint structures that bear and transmit loads, absorb energy, resist puncture and accommodate growth, respiration and/or locomotion [23], which are determined by their geometry [24-26]. In the case of bio-inspired flexible protection, natural segmented armors from fish, alligator, snake, tonicella marmoreal, pangolin, scaly foot gastropods, arapaima or armadillos are attracting an increasing amount of attention because of their unique and highly efficient protective systems to resist mechanical threats from predation, while combining hardness, flexibility, breathability, thinness, puncture-resistance and lightweight [26-31]. These natural armors, which have inspired researchers because of their diversity of geometrically structured interfaces and joints, are found in biology, for example in armored exoskeletons [32, 33], the cranium [24, 25], the turtle carapace [34] and algae [35].

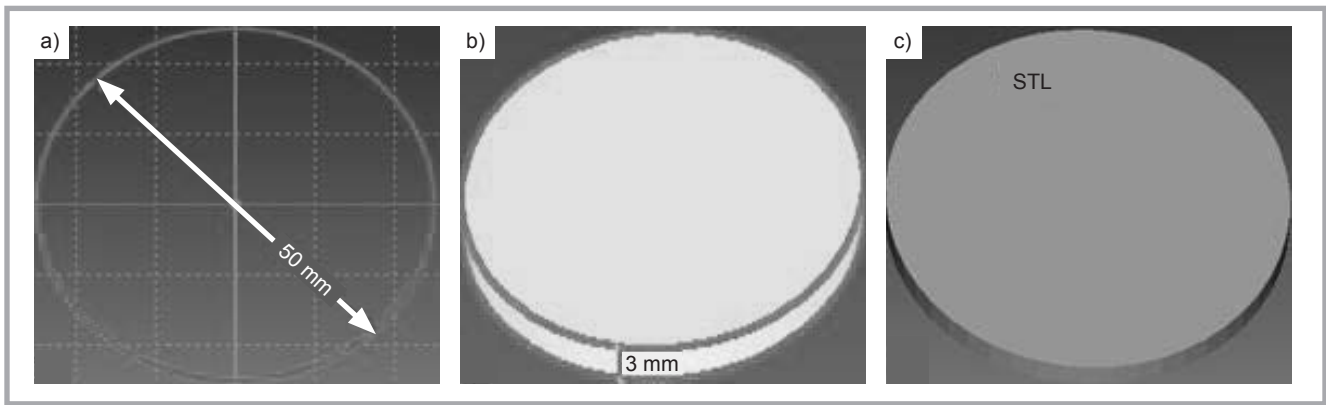Learning by imitation and further by linking all the data has probably been one of

Figure 1. *Scales designed in FreeCAD: a) sketch, b) extrusion, c) STL-file.*
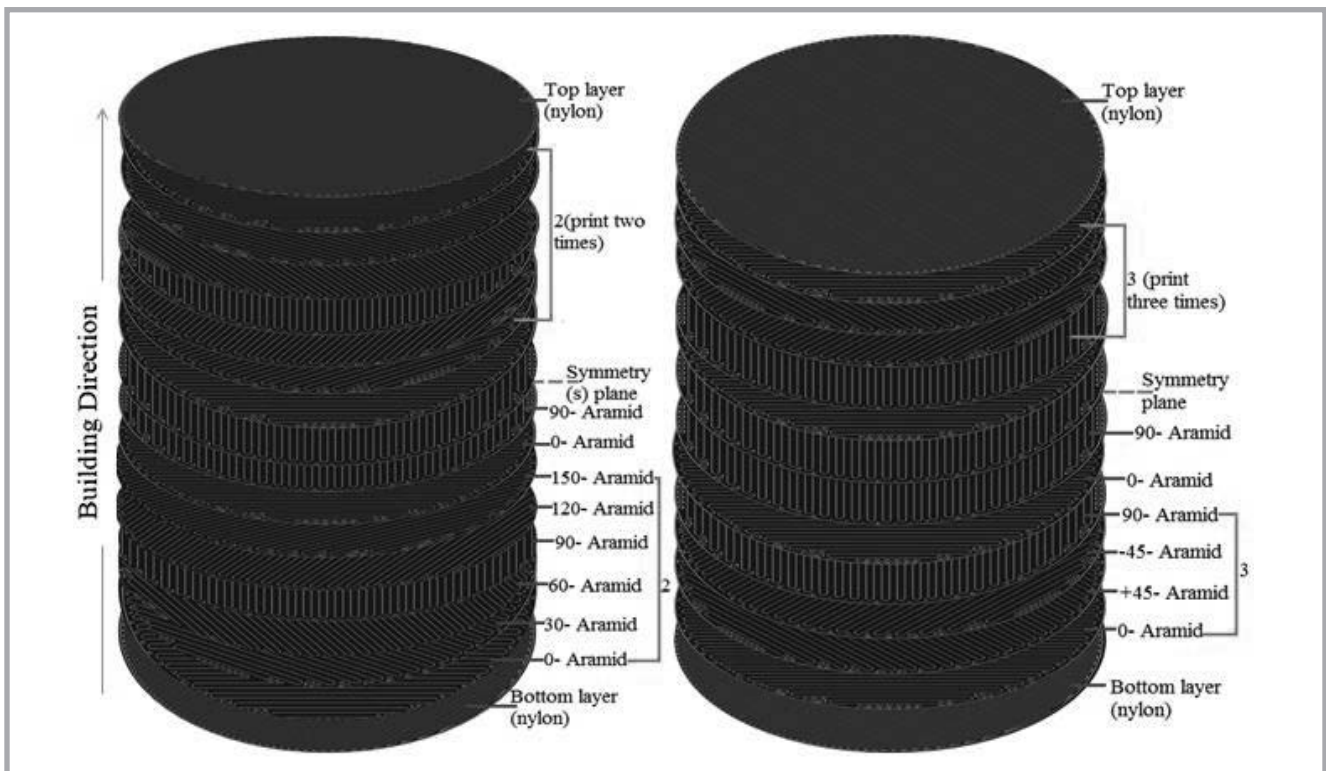

Figure 2. *Example of material arrangement and printing order of aramid layers- at filling angles $[(0/30/60/90/120/150)_2/0/90]_s$ and $[(0/+45/90/-45)_3/0/90]_s$, generated by Eiger.io.*

the most fruitful ways of development ever used. The extreme contrast of stiffness between hard scales and surrounding soft tissues gives rise to unusual and attractive mechanisms, which now serve as models for the design of bio-inspired armors. Despite this growing interest, there are few guidelines for the choice of materials, optimum thickness, size, shape and arrangement of the protective scales [36].

The aim of this research was to design and develop a three dimensional (3D) printed stab resistant armor vest based on Continuous Filament Fabrication (CFF) and inspired by natural armors. The plan was to combine a soft textile undergar-

ment and hard stab protective elements of aramid fibre-reinforced plastic (FRP). As the first step in the development of innovative stab protection clothing, the stab protection properties of 3D printed and fibre-reinforced functional elements were investigated. These were later to be used for the development of a novel vest. The performance of 3D printed aramid FRP for stab resistance was studied for 2 mm, 4 mm and 6 mm thicknesses, and the last two showed excellent performance for 25 J impact energy, while 2 mm thick scales failed the puncturing test [37]. In this research, scales were designed and developed, and their performance checked for energy level K1

(25 J) with a relatively low thickness, mass, production time and material usage as compared to the previous research result.

■ Materials and methods

Materials

3D printed stab protective elements were produced as circular scales of 3 mm thickness and 50 mm diameter from thermoplastic (nylon) and aramid fibre using a Markforged Inc.'s Mark Two Desktop 3D printer [38], with its CFF process and two printing nozzles. One nozzle operates like a typical extrusion process; it lays down a plastic filament that forms

the outer shell and the internal matrix of the part. The second nozzle deposits a continuous strand of composite fibre (example: Aramid) on every defined layer [39, 40] inside a conventional fused filament fabrication (FFF) thermoplastic part [41].

Pure nylon specimens were printed at automatic infill angles (see *Table 1*) using Markforged Inc's Mark Two software (Eiger.io). The aramid fibre infill angles shown in *Table 1* were proposed to determine the optimum protective scales with the minimum possible thickness. The materials and their arrangement in the 3D printed scales are shown in *Table 1*.

Methods

The 3D printed scale development started with designing in FreeCAD software, including meshing. The meshed design was imported to Markforged Inc.'s online software, called "Eiger.io", to select and arrange the material order, fibre alignment and composition inside the object. The Eiger-file was then transferred to the 3D printer. The scales were designed with a 3 mm thickness and 50 mm diameter (*Figure 1.a* & *1.b*), which were next converted into a standard triangle language (STL) file (*Figure 1.c*) in FreeCAD. The specimens printed with multidirectional filling angles have symmetry(s) (see *Table 1*).

Figure 2 shows the material arrangement of every layer in the 3D printed scales. The layers are arranged with different material filling angles to determine the possible optimum protection at a relatively reduced weight of the armour element (scales). The fibre angle coding was chosen in accordance with standard lamination theory for the production of composite parts. To clarify the arrangement, for example $[(0/+45/90/-45)_3/0/90]_s$ meant printing the aramid fibre three times in the order of 0, +45, 90 and -45 filling angles in each repeat, then the 0 and 90 once. Next, s the symmetry(s) was printed to complete the construction.

The sample developed from aramid has two nylon layers in each specimen, with one layer at the bottom and another at the top. Four specimens were produced for each sample as per the test method of the Association of Test Centers for Anti-attack Materials and Constructions (Vereinigung der Prüfstellenfürangriff-
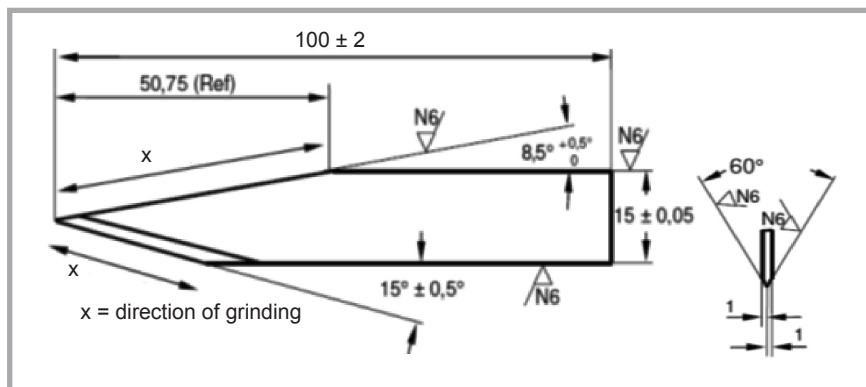

Figure 3. *Geometry of test blade P1/B (dimensions in mm) [42].*

shemmende Materialien und Konstruktionen (VPAM)) [42].

Experimental

The specimens were conditioned for a minimum duration of 24 hours at $20 \pm 1\,°C$ temperature and $65 \pm 2\%$ relative humidity [42]. The testing knife (blade), the specifications of which are shown in *Figure 3*, was attached to the drop stand to evaluate the resistance to puncture the 3D printed elements (scales). The dropping object shown in *Figure 4* has a 2.57 kg drop mass (m), 1.01m drop height and 4.44 m/s dropping speed (v), which was measured using an optical sensor to calculate the velocity right before impact. The kinetic energy (E_{kin}) applied to test the protection level of the specimens can be calculated as follows:

$$E_{kin} = \frac{1}{2} m * v^2 =$$

$$= \frac{1}{2} 2.57\ kg * (4.44\ \frac{m}{s})^2 = 25.33\ J$$

The kinetic energy used to test the specimens was 25.33 J, which is slightly higher than specified in the corresponding inspection norm (K1 = 25 J) [42], which will indicate the improved performance of the specimen if the penetration depth is lower than the one indicated in the norm.

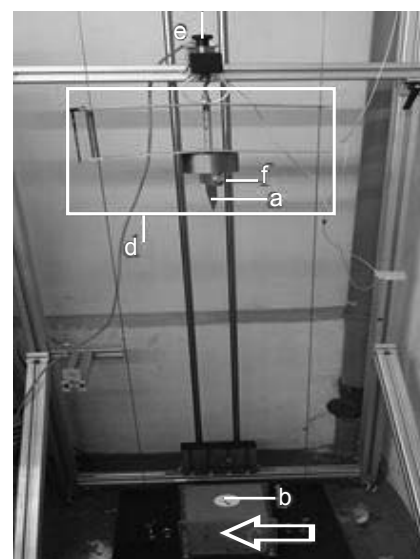The testing procedures in this study was a process in which the impact energy is

Figure 4. *Drop test stand: a) testing knife, b) specimen, c) plastilin box, d) dropping object, e) drop pressing pin, f) fixation of the knife (bolt).*

applied on the specimens to puncture and evaluate the performance of the armor scales to resist the impact energy. This includes preparation of the testing set-up, puncture testing and measurement of the penetration depth. The dropping object is released from the suspension spring and dropped on the plate (*Figure 5.a*), which is then removed (*Figure 5.b*) to measure the penetration depth of the testing knife through the scales (*Figure 5.c*). The relative alignment of the knife to the specimen is random for pure nylon and aramid

Table 1. *Material arrangement inside the 3D printed scales.*

| No.	Material	Fibre angle (in degree-°) coding	Filling layers over the total layer	Filling angles selected for
1	Nylon	$(+45/-45)_{15}$ printing angle	30 =100%	Default
2	Aramid FRP	Unidirectional(0 or 180)	28/30 =93.3%	Reduced production time
		$[(0/30/60/90/120/150)_2/0/90]_s$	28/30 =93.3%	Increasing the difficulty for the knife during its puncturing with reduced porous and varied filling angles
		$[(0/+45/90/-45)_3/0/90]_s$	28/30 =93.3%	
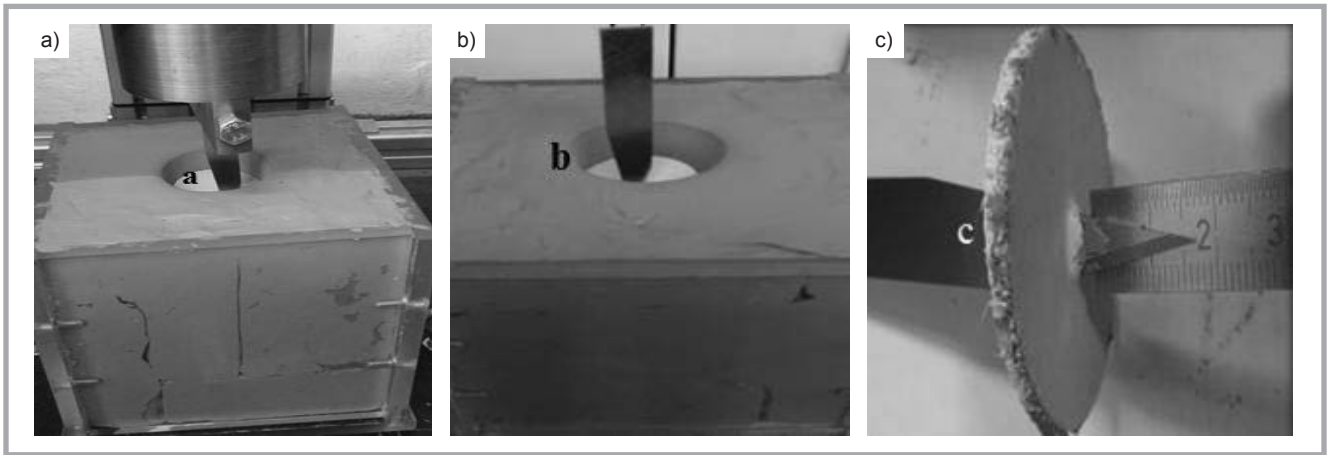
Figure 5. *Test procedure of stab resistant scales using the drop stand: a) right after puncture, b) dismantling the knife from the dropping object, c) measuring of the penetration depth of the knife.*
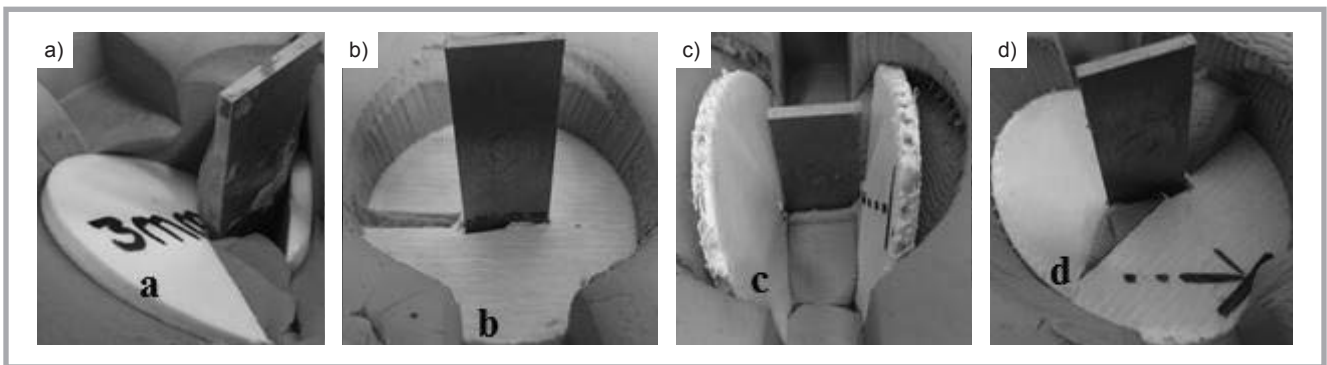

Figure 6. *Appearance of scales right after impact: a) pure nylon, b) aramid fibre angle parallel to knife, c) perpendicular to knife, d) tilted at 45° to the knife.*
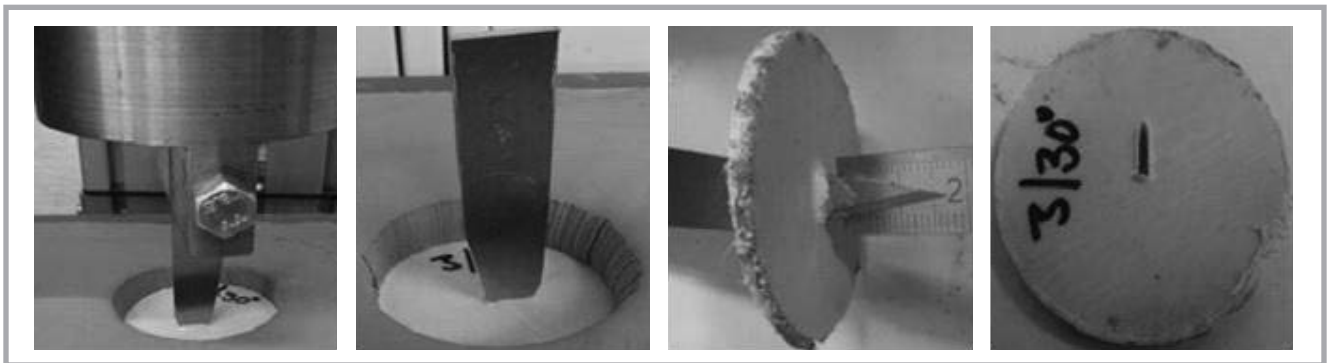

Figure 7. *Appearance and result of aramid FRP specimens at filling angle [(0/30/60/90/120/150)₂/0/90]ₛ after impact.*
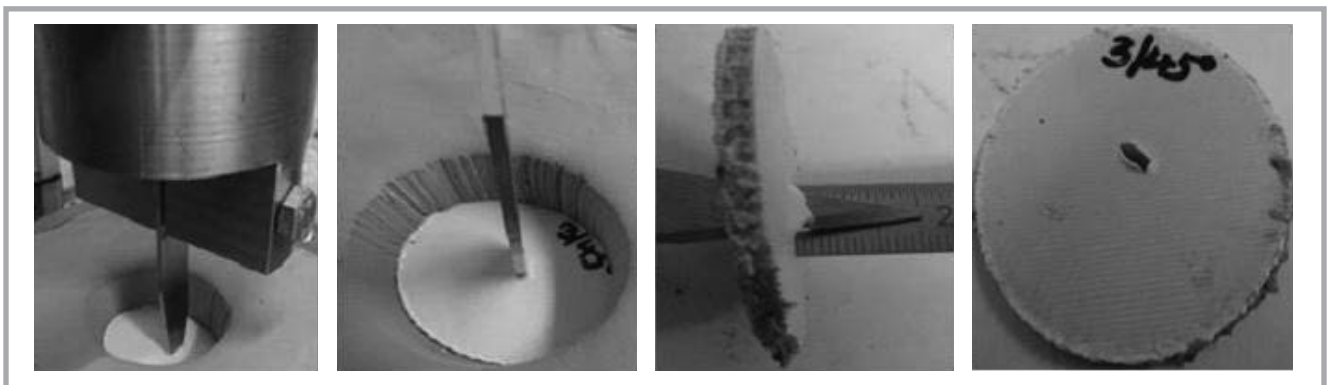

Figure 8. *Appearance and result of aramid FRP specimens at filling angle [(0/45/90/135)₂/0/90]ₛ after impact.*

printed at $[(0/30/60/90/120/150)_2/0/90]_s$ and $[(0/+45/90/-45)_3/0/90]_s$ fibre filling angles. However, the specimen made from aramid with unidirectional fibre filling was tested in three relative alignments to the knife: at a right angle, tilted at 45°, and in parallel.

Results and discussion

Protection

As indicated in the research results, the minimum organ distance from the skin is for the pleura 22 mm, pericardium 31 mm, spleen 23 mm, kidney 37 mm, thoracic aorta 64 mm, abdominal aorta 87 mm [43] and liver 22 mm [44, 45]. The maximum penetration depth of the knife should be less than the minimum distance of the organ from the skin. On the other hand, the maximum penetration depth of the knife for energy level K1 (25 J), as set by the VPAM norm, is 20 mm [42]. If the knife penetrates deeper than the maximum penetration depth set in the norm, the specimens are considered as having failed to resist the specified impact energy level K1.

As shown in *Table 2* and *Figure 6.a*, pure nylon scales are broken and completely separated after impact. The knife deeply penetrated into the plastilin (backing material) after breaking and separating the specimens printed from pure nylon. Therefore, the pure nylon specimens clearly failed to fulfil the requirements of K1.

The scales made from aramid with unidirectional fibre-reinforcement were tested, where the knife penetrated (greater than 70 mm) its entire puncturing angle with respect to the scale's filling angle directions. All specimens were broken and fully or partially separated, which leads to no protection at all.

As seen from *Figure 6.b-6.d*, unidirectional fibre filling with a specified thickness is not recommended to use for armor, even though the puncturing direction has its own insignificant effect. Therefore, specimens of 3 mm thickness made from pure nylon and unidirectional infill of aramid throughout the specimen have no or little resistance to puncturing because the penetration (>70 mm) is deeper than that allowed within the testing standard [42].

The 3D printed plates produced from aramid with a 3 mm thickness at a $[(0/30/60/90/120/150)_2/0/90]_s$ degree ar-

amid alignment and symmetrical filling significantly improved the resistance to puncture and penetration. As seen from *Figure 7*, the knife is not able to penetrate completely due to the fibre printed in multidirectional layers. Each scale has 30 printed layers, of which 28 are aramid fibre-reinforced and two (one on the top and the other on the bottom) are pure nylon. The scales withstand the impact energy of the dropping object, and the knife penetrates more deeply than that allowed (20 mm) in the norm because the fibres are arranged one over the other at different filling angles.

The 3D printed scales produced from aramid at $[(0/+45/90/-45)_3/0/90]_s$ slightly reduced the penetration depth as compared to the other samples investigated in this study, because each layer crossed over the other either diagonally or at a right angle. The other reason for the very low penetration depth of the last dropping test (11 mm depth, as seen from *Table 2*) is the plastilin becoming warmer and softer after the previous tests.

The protective elements withstand the impact energy of the dropping knife to penetrate through after puncturing for fibres arranged multi-directionally and symmetrically during designing and printing (see *Figure 7* & *Figure 8*).

In summary, scales with a unidirectional aramid fibre alignment (0° or 180°) result in low resistance to the knife during puncture. The knife penetrates easily through

the plates by more than 70 mm, which would lead to critical and fatal injuries. Some specimens are not separated after puncture, as opposite to pure thermoplastic 3D printed scales. Scales with the same thickness (3 mm) and material (aramid) give resistance to puncture and penetration due to the different fibre filling angle layers during design and 3D printing (see *Table 2*). As per VPAM KDIW 2004, the greatest permissible single stab penetration depth is 20 mm for energy level K1 (25 J) [42]. As seen in *Table 2*, the mean penetration depth of the knife through the 3D printed scales is 17.67 mm for $[(0/30/60/90/120/150)_2/0/90]_s$ and 14.67 mm for $[(0/+45/90/-45)_3/0/90]_s$ fibre filling angles. The results of this research indicate that 3D printed scales made from aramid fibre with a multidirectional filling alignment are capable of withstanding the impact energy level K1 (25 J) to save the wearer of armor made from such functional elements. The 3D printed scales investigated in this research fulfill the required protection with reduced weight and production time as compared to the previous research results [37]. The mass of the current specimen is 6.57 grams for a 1 hour and 41 minutes production time, whereas the 4 mm thick and 50 mm diameter specimen of the previous research work had a mass of 9.78 grams for a 2 hours and 13 minutes printing time, which gives a 31.5% material and 24.3% production time reduction. 3D printed protective scales made from aramid with multidirectional filling angles have an estimated area of

Table 2. Results of stab testing of aramid FRP elements.

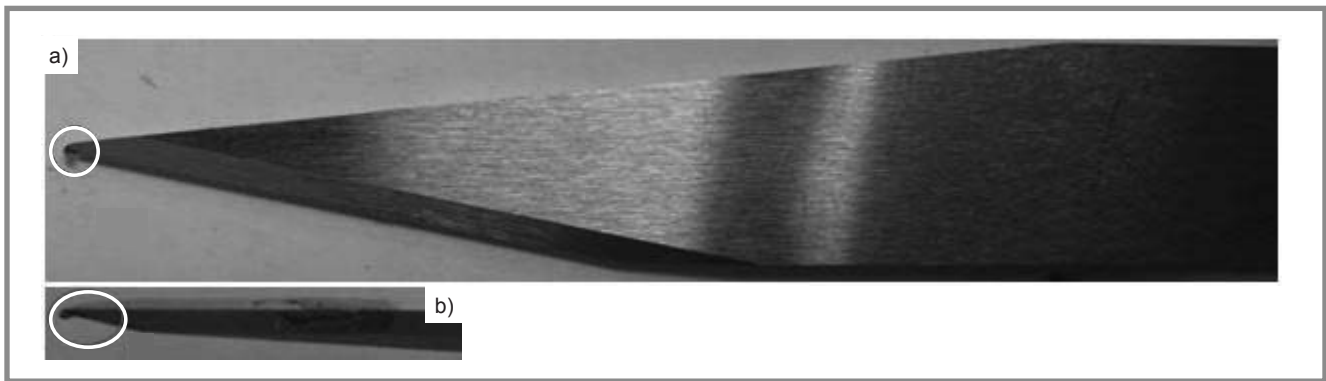| Material	Fibre angle coding	Impacting knife in filling angle direction	Trial	Penetration, mm	Mean penetration depth, mm
Nylon white	No fibres	Random	1	>70	
			2	>70	
			3	>70	
Aramid FRP	0	0	1	>70	Broken, and the penetration depth was greater than that allowed in the testing standard [42].
			2	>70	
			3	>70	
		90	1	>70	
			2	>70	
			3	>70	
		45	1	>70	
			2	>70	
			3	>70	
	$[(0/30/60/90/120/150)_2/0/90]_s$	Random	1	17	17.67
			2	17	
			3	19	
	$[(0/45/90/-45)_3/0/90]_s$	Random	1	17	14.67
			2	16	
			3	11	

Figure 9. *Damaged tip of the testing knife after impact: a) width side, b) thickness side of the testing knife.*

$A \approx 1963.5$ mm^2 with an average mass of 6.57 g, which is much lighter than the for same diameter and 2 mm thickness scale of a certified Aluminium armor (13.33 g) [46]. Therefore, 3D printed aramid protective scales provide the required protection with a relatively light weight.

The knives were bent (**Figure 9**) after puncture testing and not used to puncture repeatedly because of the high strength of the scales made with multidirectional aramid filling angles.

Conclusions

Stab protective gear would be preferred if the armors are designed for optimum protection and comfort to enable the willingness of wearers. In this research, scales were designed for armors based on bio-inspiration, and 3D printed scales were developed from aramid fibre and nylon, which are to be attached to a textile undergarment in future research activities. The minimum weight possible for energy level K1 was determined and 3D printing used for production because of its design freedom and ease of use for aramid FRP.

3D printed aramid FRP scales with a 3 mm thickness of unidirectional fibre alignment as well as multidirectional filling alignment were produced and checked for their performance. The specimens made with a unidirectional fibre alignment throughout the thickness failed, while the scales with a multidirectional fibre alignment withstood the impact energy during testing, which is supposed to be improved further by attaching elements with textiles. The scales were selected based on the natural armours of animals to provide protection with the necessary comfort parameters, such as light weight, loco-

motion, respiration and flexibility, which will be investigated further during future research activities.

The cost of production of the 3 mm thick protective plates will decrease as the ratio of nylon increases in the hybrid 3D printed scales. If the protection and production costs are optimised by developing scales of greater than 3mm thickness to reduce the ratio of aramid and increase the plastic layers, the armor will be bulkier and uncomfortable to wearers.

The design and development of 3D printed scales for a full vest, the attachment method and adhesion between scales and fabrics, computational modeling and simulation, testing of the protection and comfort of the vest, and accreditation of the novel armour are planned for future research activities.

References

1. Reiners P. Investigation about the Stab Resistance of Textile Structures, Methods for their Testing and Improvements. HAL: Université de Haute Alsace; 2016.
2. Fenne P. Protection against Knives and other Weapons. Scott RA, editor. Cambridge: Woodhead Publishing, CRC; 2005.
3. Alil L-C, Barbu C, Badea S, Ilie F. Aspects Regarding the Use of Polyethylene Fibers for Personal Armor. Eastern Michigan University, 2004.
4. Cavallaro PV. Soft Body Armor: An Overview of Materials, Manufacturing, Testing, and Ballistic Impact Dynamics. In: Division NUWC, editor.: NUWCD-NPT-TR.; 2011.
5. Laible R. Ballistic Materials and Penetration Mechanics (Methods and Phenomena, their applications in Science and Technology): Elsevier; 2012.
6. National Institute of Justice OoJP, U.S. Department of Justice. Stab Resistance of Personal Body Armor NIJ Stan-

dard–0115.00. Washington: US National Institute of Justice; 2000.
7. LaTourrette T. The Life-Saving Effectiveness of Body Armor for Police Officers. *Journal of Occupational and Environmental Hygiene* 2010; 7(10): 557-62. Epub 2010/07/17.
8. Peleg K, Rivkind A, Aharonson-Daniel L. Does Body Armor Protect from Firearm Injuries? *Journal of the American College of Surgeons* 2006; 202(4): 643-8. Epub 2006/03/31.
9. Jaslow CR. Mechanical Properties Pf Cranal Sutures. *Journal of Biomechanical* 1990; 23(4): 313-21.
10. Larsen B, Netto K, Skovli D, Vincs K, Vu S, Aisbett B. Body Armor, Performance, and Physiology During Repeated High-Intensity Work Tasks. *Military Medicine* 2012; 177(11): 1308-15. Epub 2012/12/04.
11. Greaves I. Military Medicine in Iraq and Afghanistan: A Comprehensive Review: Taylor & Francis Group, CRC Press; 2018.
12. Ricciardi R, Deuster PA, Talbot LA. Metabolic Demands of Body Armor on Physical Performance in Simulated Conditions. *Military Medicine* 2008; 173(9): 817.
13. Park H, Branson D, Petrova A, Peksoz S, Jacobson B, Warren A, et al. Impact of Ballistic Body Armour and Load Carriage on Walking Patterns and Perceived Comfort. *Ergonomics* 2013; 56(7): 1167-79. Epub 2013/05/10.
14. Chinevere TD, Cadarette BS, Goodman DA, Ely BR, Cheuvront SN, Sawka MN. Efficacy of Body Ventilation System for Reducing Strain in Warm and Hot Climates. *European Journal of Applied Physiology* 2008; 103(3): 307-14. Epub 2008/03/11.
15. Nayak R, Crouch I, Kanesalingam S, Ding J, Tan P, Lee B, et al. Body Armor for Stab and Spike Protection, Part 1: Scientific Literature Review. *Textile Research Journal* 2017; 88(7): 812-32.
16. Nayak R, Kanesalingam S, Wang L, Padhye R. Stab Resistance and Thermophysiological Comfort Properties of Boron Carbide Coated Aramid and Ballistic Nylon Fabrics. *The Journal of The Textile Institute* 2018; 110(8): 1159-68.

17. Matusiak M. Thermal Comfort Index as a Method of Assessing the Thermal Comfort of Textile Materials. *FIBRES & TEXTILES in Eastern Europe* 2010; 18, 2(79): 45-50.

18. Djongyang N, Tchinda R, Njomo D. Thermal comfort: A review paper. *Renewable and Sustainable Energy Reviews* 2010; 14(9): 2626-40.

19. Nayak R, Punj S, Chatterjee K, Behera BK. Comfort Properties of Suiting Fabrics. *Indian Journal of Fibre and Textile* 2009; 34: 122-8.

20. Philippe F, Schacher L, Adolphe DC, Dacremont C. Tactile Feeling: Sensory Analysis Applied to Textile Goods. *Textile Research Journal* 2004; 74(12): 1066-72.

21. Dempsey PC, Handcock PJ, Rehrer NJ. Impact of Police Body Armour and Equipment on Mobility. *Appl Ergon.* 2013; 44(6): 957-61. Epub 2013/05/15.

22. Legg SJ. Influence of Body Armour on Pulmonary Function. *Ergonomics* 1988; 31(3): 349-53. Epub 1988/03/01.

23. Li Y, Ortiz C, Boyce MC. Bioinspired, Mechanical, Deterministic Fractal Model for Hierarchical Suture Joints. *Physical Review E, Statistical, Nonlinear, and Soft Matter Physics* 2012; 85 (3 Pt 1): 031901. Epub 2012/05/17.

24. Pritchard J, Scott J, Girgis G. The Structure and Development of Cranial and Facial Sutures. *Journal of Anatomy* 1956; 90(1): 73-86.

25. Herring SW. Mechanical Influences on Suture Development and Patency. *Frontiers of Oral Biology* 2008; 12: 41-56. Epub 2008/04/09.

26. Dunlop JWC, Weinkamer R, Fratzl P. Artful Interfaces within Biological Materials. *Materials Today* 2011; 14(3): 70-8.

27. Vernerey FJ, Barthelat F. On the Mechanics of Fishscale Structures. *International Journal of Solids and Structures* 2010; 47(17): 2268-75.

28. Dastjerdi AK, Barthelat F. Teleost Fish Scales Amongst the Toughest Collagenous Materials. *J Mech Behav Biomed Mater*. 2015; 52: 95-107. Epub 2014/12/03.

29. Zhu D, Szewciw L, Vernerey F, Barthelat F. Puncture Resistance of The Scaled Skin from Striped Bass: Collective Mechanisms and Inspiration for New Flexible Armor Designs. *J Mech Behav Biomed Mater* 2013; 24: 30-40. Epub 2013/05/21.

30. Lin YS, Wei CT, Olevsky EA, Meyers MA. Mechanical Properties and the Laminate Structure of Arapaima Gigas Scales. *J Mech Behav Biomed Mater*. 2011; 4(7): 1145-56. Epub 2011/07/26.

31. Connors MJ, Ehrlich H, Hog M, Godeffroy C, Araya S, Kallai I, et al. Three-Dimensional Structure of the Shell Plate Assembly of the Chiton Tonicella Marmorea and Its Biomechanical Consequences. *Journal of Structural Biology* 2012; 177(2): 314-28. Epub 2012/01/18.

32. Ji B, Gao H. Mechanical Properties of Nanostructure of Biological Materials. Journal of the Mechanics and Physics of Solids 2004; 52(9).

33. Barthelat F, Tang H, Zavattieri D, Li C, Espinosa D. On the Mechanics of Mother-of-Pearl: A Key Feature In The Material Hierarchical Structure. *Journal of the Mechanics and Physics of Solids*.2007; 55(2): 306-37.

34. Krauss S, Monsonego-Ornan E, Zelzer E, Fratzl P, Shahar R. Mechanical Function of a Complex Three-Dimensional Suture Joining the Bony Elements in the Shell of the Red-Eared Slider Turtle. *Advanced Materials* 2009; 21(4): 407-12.

35. Garcia AP, Pugno N, Buehler MJ. Superductile, Wavy Silica Nanostructures Inspired by Diatom Algae. *Advanced Engineering Materials* 2011; 13(10): B405-B14.

36. Martini R, Balit Y, Barthelat F. A Comparative Study of Bio-Inspired Protective Scales Using 3D Printing and Mechanical Testing. *Acta Biomaterialia* 2017; 55: 360-72. Epub 2017/03/23.

37. Ahrendt D, Krzywinski S, Massot EJi, Krzywinski J. Hybrid Material Designs by the Example of Additive Manufacturing for Novel Customized Stab Protective Clothing. Light Weight Armour Group for Defense and Security; Roubaix, France2019. p. 286-94.

38. Markforged. Markforged the Mark Two Desktop 3D Printer. Germany: Markforged, Inc; 2019 [cited 2020 05 April]; Available from: https://markforged.com/mark-two/.

39. Langau L. What is Continuous Fiber Fabrication (CFF)? Make Parts Fast, A Design World Resource2017.

40. Dean A. A Review on Markforged Mark Two: the basics of how it works. DEVELOP3D. 2016.

41. 3D Printer Types & Technologies [database on the Internet]. Markforged. 2019. Available from: https://markforged.com/learn/3d-printer-types-technologies/.

42. Office of the Deutsche Hochschule der Polizei Polizeitechnisches Institut. Test Standard Stab and Impact Resistance. Requirements, classifications and test procedures. Deutschland: Vereinigung der Prüfstellen für angriffshemmende Materialien und Konstruktionen (VPAM); 2011.

43. Connor SEJ, Bleetman A, Duddy MJ. Safety Standards for Stab-Resistant Body Armour: A Computer Tomographic Assessment of Organ to Skin Distances. International Journal of the Care of the Injured 1998; 29(4): 297-9.

44. Su S, Wang W, Nadebaum D, Nicoll A, Sood S, Gorelik A, et al. Skin-Liver Distance and Interquartile Range-Median Ratio as Determinants of Interoperator Concordance in Acoustic Radiation Force Impulse Imaging. *Journal of Medical Ultrasound* 2019; 27(4): 4.

45. Shen F, Zheng R-D, Shi J-P, Mi Y-Q, Chen G-F, Hu X, et al. Impact of Skin Capsular Distance on the Performance of Controlled Attenuation Parameter in Patients with Chronic Liver Disease. *Liver International* 2015; 2015: 9. John Wiley & Sons Ltd.

46. Aalco. Weight calculator. England & Wales: Aalco metals limited; 2020; Available from: http://www.aalco.co.uk/online-tools/weight-calculator/.

Clothing-Body 2021 INTERACTION

JUNE, 2 – 3

Joint International Conference

www.clothing-body-interaction.eu